ICESat's new perspective on ice shelf rifts: The vertical dimension

H. A. Fricker, J. N. Bassis, and B. Minster

Institute of Geophysics and Planetary Physics, Scripps Institution of Oceanography, La Jolla, California, USA

D. R. MacAyeal

Department of Geophysical Sciences, University of Chicago, Chicago, Illinois, USA

Received 28 October 2005; accepted 28 October 2005; published 1 December 2005.

[1] The small footprint (~70 m) and ~172 m along-track spacing of the Geoscience Laser Altimeter System (GLAS) on the Ice, Cloud and land Elevation Satellite (ICESat) provides unprecedented horizontal resolution for a satellite altimeter. This enables ICESat to map many previously unresolved features on ice shelves, such as crevasses, rifts, grounding zones and ice fronts. We present examples of ICESat-derived elevation data showing topography over rifts on the Amery and Ross ice shelves, widths of rifts and as estimates of the thickness of mélange (a collection of ice and snow trapped inside the rifts). We show that mélange thickness remains constant over the ICESat data period and tends to be thicker in older rifts. We validate the ICESat-derived mélange depth estimate with an *in situ* measurement on the Ross Ice Shelf. **Citation:** Fricker, H. A., J. N. Bassis, B. Minster, and D. R. MacAyeal (2005), ICESat's new perspective on ice shelf rifts: The vertical dimension, *Geophys. Res. Lett.*, *32*, L23S08, doi:10.1029/2005GL025070.

1. Introduction

[2] Satellite radar altimeters (RA) have vastly improved our knowledge of Antarctic ice sheet surface topography, with the ERS and Envisat RA's providing data since 1991. Launched in January 2003, ICESat, carries the first laser altimeter to operate in a polar orbit, and started a new era in ice sheet altimetry. GLAS has higher accuracy, along-track resolution and improved tracking over ice than the ERS/Envisat RAs. It also provides coverage to 86°S (cf. 81.5°S), which includes all of the Antarctic ice shelves. The increased resolution, tracking and coverage means that "small-scale" features of ice shelves, e.g., rifts, ice fronts and grounding zones, can be studied for the first time with satellite altimetry. Previous RA studies tend to neglect these features, because the data are typically averaged over large areas, and because the large RA footprint (~2–3 km over ice does not resolve such small features. ICESat's high along-track resolution (~65 m footprint and ~172 m spacing) reveals exquisite topographic detail over features such as crevasses, through-cutting rifts, ice shelf margins, ice fronts, icebergs and grounding zones. In this paper we focus on rifts; another paper in this Special Section considers icebergs [*Scambos et al.*, 2005]. We present ICESat profiles over a selection of rifts in Antarctica, and use the data to estimate the mélange thickness. This is a novel application of altimeter data over ice shelves, which demonstrates the powerful capability of ICESat for monitoring features that are too small to be resolved by other altimetry systems.

2. Ice Shelf Rifts

[3] Rifts in Antarctic ice shelves are fractures that penetrate the full ice shelf thickness. Satellite imagery enables us to examine the surface expressions of rifts. Some rifts are formed centuries earlier at locations far upstream and then are advected toward the ice front. Such "relic" rifts may provide an important fingerprint of past ice shelf conditions [*Fahnestock et al.*, 2000]. These rifts have often become inactive and have slowed or stopped propagating completely by the time they reach the ice shelf front. Other rifts are believed to have initiated in the recent past in response to high glaciological stresses at the ice shelf front [*Joughin and MacAyeal*, 2005; *Bassis et al.*, 2005]. These rifts propagate and can eventually form the detachment boundaries for the calving of large tabular icebergs. Rift propagation rates on the Amery Ice Shelf have been shown to be seasonal [*Fricker et al.*, 2005] indicating that it is possible that they might be sensitive to a changing climate. Rifts are typically filled with a collection of different ice types called ice mélange [*MacAyeal et al.*, 1998], which several authors have suggested may play an important role in controlling propagation rates [e.g., *Larour et al.*, 2004; *Bassis et al.*, 2005; *Hulbe et al.*, 1998]. However, its exact role is unknown, and little is known about its composition and properties, especially how it effects rift propagation. Some authors have suggested that mélange acts as a glue which holds the rift walls together and resists further propagation [*Larour et al.*, 2004; *Hulbe et al.*, 1998], while others have suggested that the blocks of ice which fall into the rift are a component of the driving stresses, wedging the rift open [*Bassis et al.*, 2005].

3. ICESat Data

[4] We used ICESat data from the 91-day repeat phases: Laser 2a, 10/04/03–11/18/03 (Release 21); Laser 2b, 02/17/2004–03/21/2004 (Release 16); Laser 2c: 05/18/04–06/21/04 (Release 17); Laser 3a, 10/03/04–11/08/04 (Release 18); Laser 3b, 02/17/05–03/22/05 (Release 19). We combined data from the GLA01 Global Altimetry Data Product, the GLA05 Global Waveform-based Range Corrections Data Product and the GLA12 Antarctic and Greenland Ice Sheet Data Product.

[5] No data filtering—i.e., no rejection of data records—for clouds was performed since we wished to retain infor-

0094-8276/05/2005GL025070$05.00

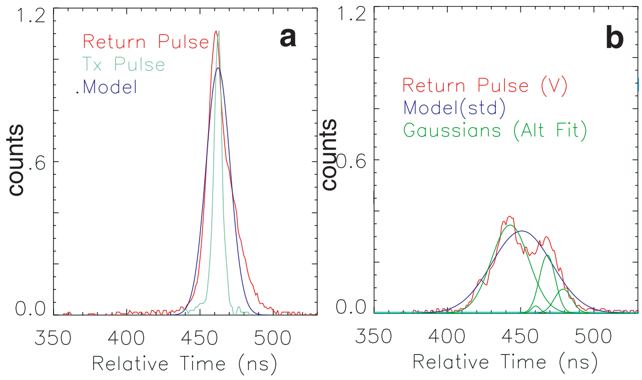

Figure 1. Example ICESat pulses from (a) smooth ice shelf surface, T_x = transmitted pulse; (b) an ice shelf rift. Both plots show return pulse and "standard" fit, and Figure 1b shows "alternate" fits.

mation over rough surfaces, and we found that the filters used by *Smith et al.* [2005] removed many of these data. In the "standard fit" process used to estimate the GLA12 elevation, the elevation corresponds to the centroid of a Gaussian fit to the return pulse (Figure 1a). Across most of the ice shelves there is only one peak in the return pulse, giving an unambiguous estimation of the elevation. Across rifts and other complex surfaces, multiple reflecting surfaces within the GLAS footprint yield multiple peaks in the return pulse (Figure 1b). In such cases, an "alternate" fit with up to six Gaussians is used to estimate the set of elevations within the footprint, and these fits can provide valid information about the small-scale topography with wavelength smaller than the footprint diameter. The alternate fit data are given in GLA05, however, they are known to contain errors in Release 18 and lower, so were not available for Laser 2b, Laser 2c or Laser 3a at the time of writing.

4. Study Regions

[6] We selected two of Antarctica's major ice shelves for this study: the Amery Ice Shelf (AIS) and Ross Ice Shelf (RIS). The AIS has a well-developed rift system near its front, which consists of two non-propagating longitudinal-to-flow rifts (L1 and L2) and two propagating transverse-to-flow rifts (T1 and T2; Figure 2a) [*Fricker et al.*, 2005]. The tip of rift T2 is an ICESat Target of Opportunity (TOO), whereby the spacecraft is pointed off-nadir so as to hit the same geographical location when its planned ground-track falls within 50 km.

[7] Since RIS is further south than AIS, the track separation of ICESat is smaller, enabling more detailed mapping. On RIS most of the rifts are close to the ice front and are transverse-to-flow (Figure 2b). There is a ~160 km rift near Roosevelt Island (labeled "A" on Figure 2b), which is believed to originate from the same fracture-inducing zone as the rift that became the B-15 iceberg in March 2000 [*Lazzara et al.*, 1999], as well as others closer to the center of the front (B, C). There are two large bow-shaped rifts (D and E) that may have formed downstream of a major slowing of Mercer Ice Stream (M. A. Fahnestock, personal communication, 2005). Feature F is old mélange that is still attached to the ice front, left behind after the C-19 calving in May 2002.

5. Results

5.1. Mélange Thickness Estimates

[8] The first ICESat elevation profile along the AIS TOO ascending track (Figure 2a) was acquired 18 October 2003 (Track 1307, Laser 2a). Figure 3a shows this profile and estimated ice draft assuming hydrostatic equilibrium with the following densities: 1028 kg m^{-3} for sea-water, 876 kg m^{-3} for ice shelf ice and 865 kg m^{-3} for mélange [*King*, 1994]. Over the ice shelf surface, only elevation and thickness estimates derived from the GLA12 standard fit are shown. Over the rifts, estimates corresponding to the six GLA05 alternate fit peaks are also shown, color-coded according to the Gaussian to which they correspond. We estimated freeboard elevation by subtracting the mean ocean elevation seaward of the ice front, from 13 GLAS footprints. This eliminates both tidal effects and the need for applying a geoid-ellipsoid elevation correction. The mean mélange freeboard elevation is 14.5 ± 4.7 m for L1 and 12.5 ± 3.8 m for T2; derived mélange thickness estimates (using the same densities given above) were 98.2 ± 31.4 m for T2 and 85.1 ± 25.6 m for L1. Figure 3b shows mélange thickness estimates (from GLA12 only) for L1 and T2 from seven repeats of the same TOO Track. Figure 3c shows estimated mélange thicknesses for both rifts for all passes: where Release 19 and higher data were available (Laser 2a and Laser 3b), these estimates included GLA05 alternate fit data. This figure shows that there are no significant changes in mélange thickness in either rift over the period covered by ICESat.

[9] We also computed mélange thickness on the RIS, where we were able to validate the estimate. In October

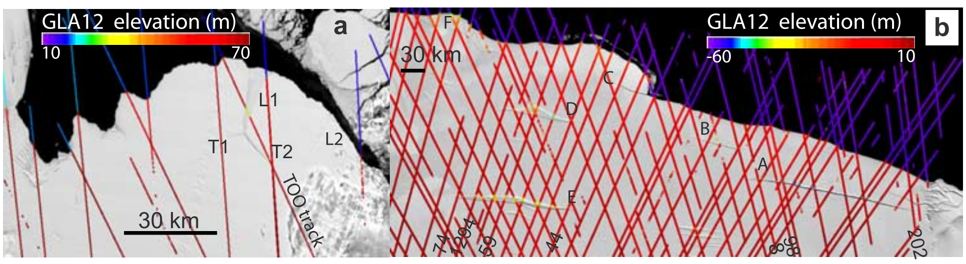

Figure 2. (a) MODIS image (23 October 2003) over AIS front; (b) MODIS Mosaic of Antarctica [*Bohlander et al.*, 2004] over RIS front. ICESat Laser 2a tracks are overlaid, and those discussed elsewhere are labeled by track number.

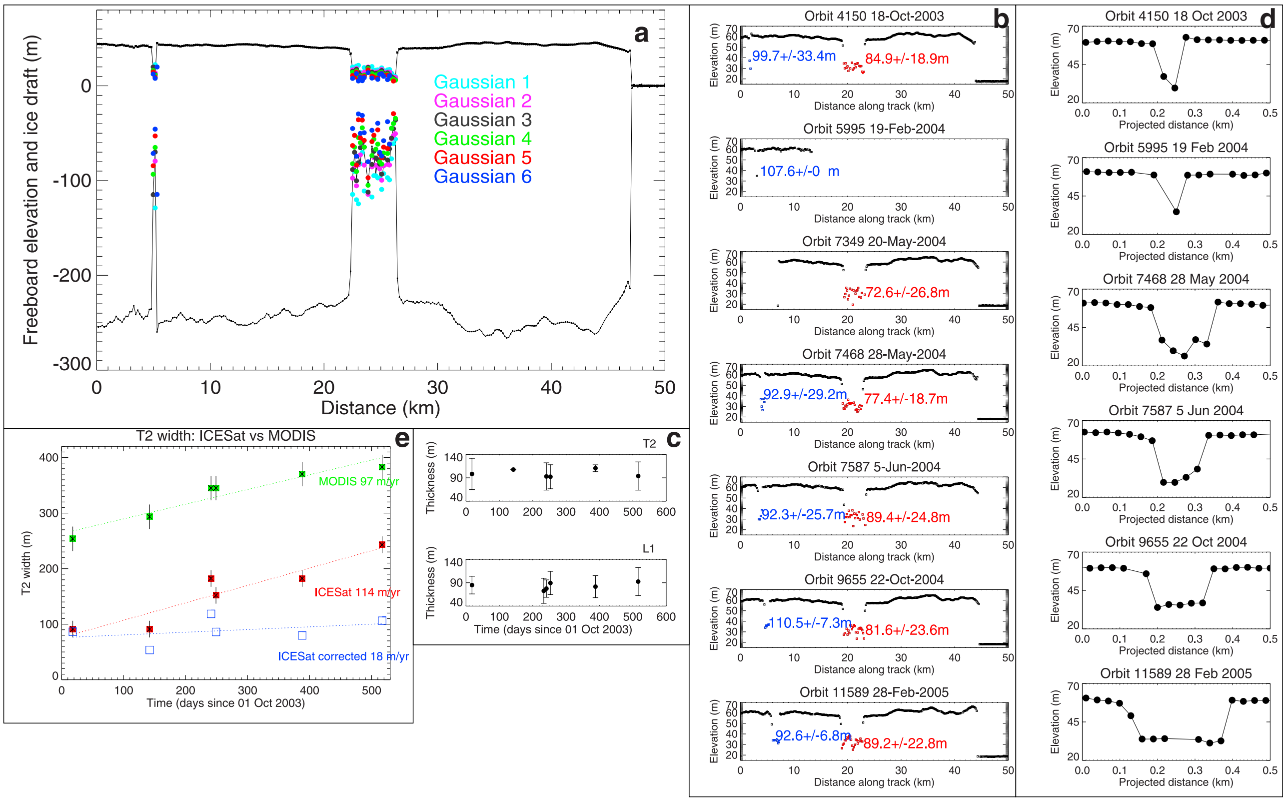

Figure 3. (a) ICESat elevation profile along Laser 2a TOO track; (b) repeat passes of AIS TOO track, with estimated mélange thicknesses; (c) time series of mélange thicknesses for T2 and L1; (d) T2 rift opening; (e) ICESat vs MODIS widths for T2.

2004, a field party to the RIS rift E dropped and marked a climbing rope inside the rift at the location of ICESat Track 1288, 10 days after ICESat had acquired data along this track during Laser 3a (Figure 3a, at the location of label "C"). The estimate of the rift depth using the climbing rope was 30.6 m and the estimate from ICESat (GLA12) was 29.3 m, a remarkable agreement considering the relative differences and difficulties of the two measurement approaches.

5.2. Rift Widening

[10] Repeats across rift T2 suggest evidence of rift widening (Figure 3d). Here, the x-axis is perpendicular distance across the rift, projected onto the normal to the rift; the distance between ICESat points in this projection is ~30 m. Ice motion has been removed to align each plot. On 18 October 2003 two pulses reflected from inside the rift, suggesting a width of ~90 m. On 28 February 2005 eight pulses (two of them were invalid) inside the rift suggests a width of ~270 m. Some of this widening is due to advection of the rift downstream between passes. To estimate this contribution, we used ice velocities determined by GPS during a 2002–2003 field campaign [*Bassis et al.*, 2005] to subtract the distance the rift had moved between each pass. By plotting these "ice-velocity-corrected" tracks on a MODIS image from 23 October 2003, we were able to estimate the width of the rift at the intersection point for each pass (Figure 3e). From the MODIS widths, we estimate that the apparent change in rift width due to the track intersecting the rift at different locations is approximately 26 cm/day (97 m/yr). The opening rate calculated from the ICESat data is 31 cm/day (114 m/yr), therefore we believe that part of the signal we observe is true rift widening. The resultant opening rate of 18 m/yr is an order of magnitude smaller than opening rates reported for rifts on Ross Ice Shelf near Roosevelt Island (150–250 m/yr), observed SAR imagery by *Joughin and MacAyeal* [2005]. This is most likely because we are measuring the widths very close to the rift tip, where the widening is at its smallest. We also see evidence of rift widening in repeat profiles across rifts on RIS (e.g., Track 44, Figure 4e; see Figure 2b for location).

5.3. Rift Topography

[11] Another feature of rifts that ICESat is able to resolve is the topography of the rift flanks. For example, a profile across rift T2 reveals uplift on both sides (Figure 3a), which is asymmetrical such that the northern (seaward) side is higher in elevation than the southern (landward) side. This elevation difference is consistent with observations made in the field in January 2003, when a 1–2 m elevation offset on the northern side of T2 was noted. The repeat TOO passes of T2 show that as the rift propagates the topography along the rift changes, e.g., in the 28 February 2005 profile, the topography on the southern rift flank has become gently sloped. Similar topography across the rift flanks is seen on RIS. Figure 4a shows stacked profiles across rift A. The spatial pattern of the structure of the rift flank topography shows that the asymmetry is largest at a distance of 2–3 km from the rift tip. Near the center of the rift both sides are typically uplifted by similar amounts. We propose that the observed uplift is related to the rifting process but is

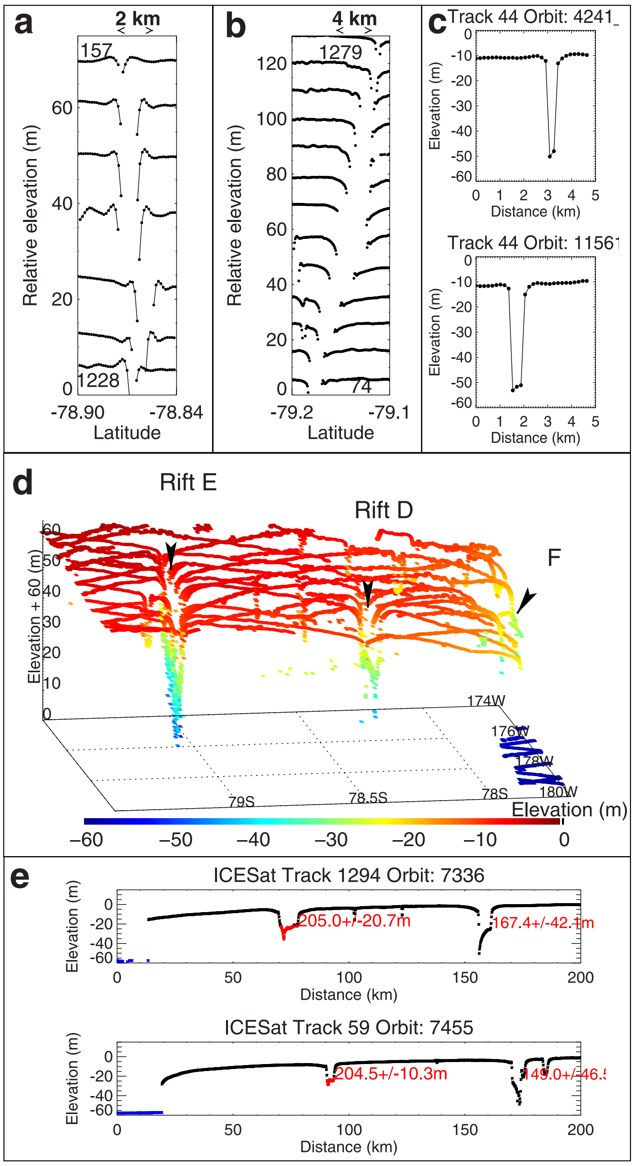

Figure 4. (a) ICESat Laser 2a profiles across a) Rift A (active) and (b) Rift E (relic) - adjacent profiles are offset by 10 m in elevation and first and last profiles are labeled by track number (see Figure 2b); (c) Laser 3a and 3a profiles across Rift C; (d) Laser 2a profiles across Rifts D and E and ice front; (e) Laser 3c profiles across Rifts E and D (see Figure 2b).

obscured over time by other processes (e.g., snow drift build-up, erosion and ice-shelf talus infall). The topography across relic rifts D and E supports this theory: profiles across the rifts walls show a steepening on both sides into the rift with some uplift on the northern side (Figures 4b, 4c and 4d). This implies that the topography across a rift might tell us about the age and recent activity of the rift, in addition to being an indicator of the mechanical process of rifting.

[12] As an example of how extensively features can be mapped on RIS, a three-dimensional (3-D) rendition of the topography across rifts D and E is shown in Figure 4c. An individual profile across these rifts (Figure 4e; Track 1294; see Figure 2b for location) reveals an asymmetry in the shape of the mélange trapped inside them, and also show that the mélange in the older, downstream rift is substantially thicker (~204 m vs. ~150 m). We believe that the top surface of mélange in these rifts is due to wind-blown snow, and that its surface pattern is asymmetric because snow is primarily deposited on the windward side. Near the center of Rift E there is a change in the sense of the asymmetry (Figure 4e; Track 59; see Figure 2b for location), which is possibly due to the presence of two smaller rifts upstream, into which wind-blown snow gets deposited first (see Figure 2). The residual mélange platform from the C-15 calving (F in Figure 2b) is indicated in Figure 4c. Also evident in this figure is a significant slope towards the RIS front, which is a likely due to local basal melting along the front of the ice shelf [*Jenkins and Doake*, 1991].

6. Summary

[13] We have demonstrated the unique capability of the GLAS instrument on ICESat to provide topographic information over features that are too small to be visible with previous altimeter instruments: ice shelf rifts. For the first time we are able to study in detail the topographic form of ice shelf rifts using satellite altimeter data. Since ice shelf rifting is a 3-D process it is important to gather both vertical and lateral information: ICESat combined with other satellite imagery provides this critical 3-D information. ICESat also allows us to make measurements of the thickness of mélange filling rifts, a potentially an important factor in ice shelf rifting. Rifts may be sensitive indicators of climate change and ice dynamics, therefore monitoring them is an important part of ice sheet change detection.

[14] **Acknowledgments.** This work was supported by NASA contract NAS5-99006 and NSF grant OPP-0337838. We thank NASA's ICESat Science Project and the NSIDC for distribution of the ICESat data, see http://icesat.gsfc.nasa.gov and http://nsidc.org/data/icesat. We would like to acknowledge J. DiMarzio, D. Hancock, K. Barbieri, D. Harding, J. Saba, A. Borsa, C. Shuman, V. Suchdeo, R. Coleman, T. Scambos, M Fahnestock and R. Warner for helpful input. Our sincere thanks to K. Brunt, B. Brunner and L. Littrel (latter two being part of the Raytheon Polar Services field safety team) and rest of the Ross Ice Shelf 2003 field team. Fieldwork supported by NSF OPP-0229546.

References

Bassis, J. N., R. Coleman, H. A. Fricker, and J. B. Minster (2005), Episodic propagation of a rift on the Amery Ice Shelf, East Antarctica, *Geophys. Res. Lett.*, *32*(6), L06502, doi:10.1029/2004GL022048.

Bohlander, J., T. Scambos, T. Haran, and M. Fahnestock (2004), A new MODIS-based mosaic of Antarctica: MOA, *Eos Trans. AGU*, *85*(47), Fall Meet. Suppl., Abstract C31B-0319.

Fahnestock, M. A., T. A. Scambos, R. A. Bindschadler, and G. Kvaran (2000), A millennium of variable ice flow recorded by the Ross Ice Shelf, Antarctica, *J. Glaciol.*, *46*, 652–664.

Fricker, H. A., N. W. Young, R. Coleman, J. N. Bassis, and J.-B. Minster (2005), Multi-year monitoring of rift propagation on Amery Ice Shelf, East Antarctica, *Geophys. Res. Lett.*, *32*(2), L02502, doi:10.1029/2004GL021036.

Hulbe, C. L., E. Rignot, and D. R. MacAyeal (1998), Comparison of ice-shelf creep flow simulations with ice-front motion of Filchner-Ronne Ice Shelf, Antarctica, detected by SAR interferometry, *Ann. Glaciol.*, *27*, 182–186.

Jenkins, A., and C. S. M. Doake (1991), Ice-ocean interaction on Ronne Ice Shelf, Antarctica, *J. Geophys. Res.*, *96*, 791–813.

Joughin, I., and D. R. MacAyeal (2005), Calving of large tabular icebergs from ice shelf rift systems, *Geophys. Res. Lett.*, *32*, L02501, doi:10.1029/2004GL020978.

King, E. C. (1994), Observations of a rift in the Ronne Ice Shelf, Antarctica, *J. Glaciol.*, *40*, 187–189.

Larour, E., E. Rignot, and D. Aubry (2004), Modelling of rift propagation on Ronne Ice Shelf, Antarctica, and sensitivity to climate change, *Geophys. Res. Lett.*, *31*, L16404, doi:10.1029/2004GL020077.

Lazzara, M. A., K. C. Jezek, T. A. Scambos, D. R. MacAyeal, and C. J. van der Veen (1999), On the recent calving of icebergs from the Ross Ice Shelf, *Polar Geogr.*, *23*, 201–212.

MacAyeal, D. R., E. Rignot, and C. Hulbe (1998), Ice shelf dynamics near the front of the Filchner Ronne Ice Shelf, East Antarctica, revealed by SAR interferometry: Model/interferogram comparison, *J. Glaciol.*, *44*, 419–428.

Scambos, T., O. Sergienko, A. Sargent, D. MacAyeal, and J. Fastook (2005), ICESat profiles of tabular iceberg margins and iceberg breakup at low latitudes, *Geophys. Res. Lett.*, *32*, L23S09, doi:10.1029/2005GL023802.

Smith, B. E., C. R. Bentley, and C. F. Raymond (2005), Recent elevation changes on the ice streams and ridges of the Ross Embayment from ICESat crossovers, *Geophys. Res. Lett.*, *32*, L21S09, doi:10.1029/2005GL024365.

J. N. Bassis, H. A. Fricker, and B. Minster, IGPP, Scripps Institution of Oceanography, La Jolla, CA 92093, USA. (hafricker@ucsd.edu)

D. R. MacAyeal, Department of Geophysical Sciences, University of Chicago, Chicago, IL 60637, USA.